4-*O*-methylation of glucuronic acid in *Arabidopsis* glucuronoxylan is catalyzed by a domain of unknown function family 579 protein

Breeanna R. Urbanowicz[a,b,1], Maria J. Peña[a,b,1], Supriya Ratnaparkhe[a,2], Utku Avci[a,b], Jason Backe[a,b], Heather F. Steet[a], Marcus Foston[b,c], Hongjia Li[b,d], Malcolm A. O'Neill[a,b], Arthur J. Ragauskas[b,c], Alan G. Darvill[a,b,e], Charles Wyman[b,d], Harry J. Gilbert[a,3], and William S. York[a,b,e,4]

[a]Complex Carbohydrate Research Center and [e]Department of Biochemistry and Molecular Biology, University of Georgia, Athens, GA 30602; [b]BioEnergy Science Center, Oak Ridge National Laboratory, Oak Ridge, TN, 37831; [c]Department of Chemistry and Biochemistry, Georgia Institute of Technology, Atlanta, GA 30332; and [d]Center for Environmental Research and Technology, University of California, Riverside, CA 92507

Edited by Chris R. Somerville, University of California, Berkeley, CA, and approved July 20, 2012 (received for review May 11, 2012)

The hemicellulose 4-*O*-methyl glucuronoxylan is one of the principle components present in the secondary cell walls of eudicotyledonous plants. However, the biochemical mechanisms leading to the formation of this polysaccharide and the effects of modulating its structure on the physical properties of the cell wall are poorly understood. We have identified and functionally characterized an *Arabidopsis* glucuronoxylan methyltransferase (GXMT) that catalyzes 4-*O*-methylation of the glucuronic acid substituents of this polysaccharide. AtGXMT1, which was previously classified as a domain of unknown function (DUF) 579 protein, specifically transfers the methyl group from S-adenosyl-L-methionine to *O*-4 of α-D-glucopyranosyluronic acid residues that are linked to *O*-2 of the xylan backbone. Biochemical characterization of the recombinant enzyme indicates that GXMT1 is localized in the Golgi apparatus and requires Co^{2+} for optimal activity in vitro. Plants lacking GXMT1 synthesize glucuronoxylan in which the degree of 4-*O*-methylation is reduced by 75%. This result is correlated to a change in lignin monomer composition and an increase in glucuronoxylan release during hydrothermal treatment of secondary cell walls. We propose that the DUF579 proteins constitute a previously undescribed family of cation-dependent, polysaccharide-specific *O*-methyl-transferases. This knowledge provides new opportunities to selectively manipulate polysaccharide *O*-methylation and extends the portfolio of structural targets that can be modified either alone or in combination to modulate biopolymer interactions in the plant cell wall.

recalcitrance | biosynthesis

The evolution of vascular tissues with rigid secondary cell walls was a critical adaptive event in the history of land plants (1). These tissues are required to transport water and nutrients throughout the plant body and provide the mechanical strength to sustain the extensive upright growth needed to compete for sunlight (1). Secondary walls have also had an impact on human life, as they are a major component of wood (2) and are a source of nutrition for livestock (3). Moreover, these walls account for the bulk of renewable biomass that can be converted to fuel and added-value chemicals (4). Such ever-increasing demands on plants for fuel and for food has led to a renewed interest in developing crops with secondary walls engineered to improve their agronomic value (5). However, progress in this area is limited by our incomplete understanding of the mechanisms of cell wall biosynthesis (6–8).

Cellulose, lignin, and 4-*O*-methyl glucuronoxylan (GX) are the principle components present in the secondary walls of eudicotyledons (6). These polymers interact with themselves and with each other via covalent and noncovalent bonds to form a macromolecular network that determines the biological and physical properties of the secondary wall. Advances in understanding cellulose and lignin biosynthesis (9, 10) and some of the genetic factors that regulate secondary wall formation (11) have begun to provide insight into wall structure and assembly. Much less is known about GX synthesis and the mechanisms by which this polysaccharide interacts with cellulose and lignin to form a functional wall (6).

In hardwoods and in mature stems of the model plant *Arabidopsis thaliana*, GX has a backbone composed of 1,4-linked β-D-xylosyl (Xyl) residues that are often substituted at *O*-2 with α-D-glucuronic acid (GlcA) or 4-*O*-methyl α-D-glucuronic acid (4-*O*-MeGlcA) and at *O*-2 and *O*-3 with acetyl groups (6, 12) (Fig. 1). *Arabidopsis* GX has approximately one uronic acid residue for every eight Xyl residues and a GlcA to 4-*O*-MeGlcA ratio of 1:3 (13). 4-*O*-MeGlcA has been identified in all GXs that have been isolated from vascular plants (12). In contrast, the avascular moss *Physcomitrella patens*, which does not form lignified secondary cell walls, produces a GX that lacks *O*-methyl-etherified GlcA (14), suggesting that *O*-methylation of GXs establishes key structural features of the secondary cell walls of vascular plants.

GX synthesis requires the coordinated action of numerous enzymes, including glycosyltransferases (GTs), *O*-acetyl transferases, and *O*-methyl transferases (OMTs) (6, 13). Genetic approaches have provided limited insight into the mechanisms of GX synthesis, as plants carrying mutations in many of the putative xylan synthesis genes have severe growth and developmental defects related to abnormal secondary wall formation (13, 15, 16). Nevertheless, the protein encoded by *Glucuronic Acid Substitution of Xylan* (*GUX)1*, a Family 8 GT responsible for adding the glucuronosyl substituent onto the GX backbone, has been isolated and biochemically characterized in vitro (17). Much less is known about the other GTs involved in secondary wall GX synthesis (8, 13, 18–20). No xylan *O*-acetyl or OMT has been isolated nor have the genes that encode these enzymes been identified. Thus, there is a lack of information regarding the biochemical mechanisms by which *O*-acetyl and *O*-methyl substituents are added to GX and how these substituents affect the structure and function of the secondary wall.

Numerous cation-dependent plant OMTs have been identified and shown to catalyze the transfer of the methyl group from *S*-adenosyl methionine (SAM) to secondary metabolites (21–23). Such methylation expands the chemical diversity of these low

Author contributions: B.R.U., M.J.P., C.W., H.J.G., and W.S.Y. designed research; B.R.U., M.J.P., S.R., U.A., J.B., H.F.S., M.F., and H.L. performed research; B.R.U., M.J.P., H.F.S., M.F., H.L., M.A.O., A.J.R., A.G.D., C.W., H.J.G., and W.S.Y. analyzed data; and B.R.U., M.J.P., M.A.O., and W.S.Y. wrote the paper.

The authors declare no conflict of interest.

This article is a PNAS Direct Submission.

[1]B.R.U. and M.J.P. contributed equally to this work.

[2]Present address. Department of Biotechnology Institute of Chemical Technology, Deemed University, Centre for Energy Biosciences, Matunga, Mumbai 400 019, India.

[3]Present address. Institute for Cell and Molecular Biosciences, University of Newcastle upon Tyne, Newcastle upon Tyne NE2 4HH, United Kingdom.

[4]To whom correspondence should be addressed. E-mail: will@ccrc.uga.edu.

This article contains supporting information online at www.pnas.org/lookup/suppl/doi:10.1073/pnas.1208097109/-/DCSupplemental.

Downloaded at ESKISEHIR OSMANGAZI UNIVERSITY on November 10, 2021

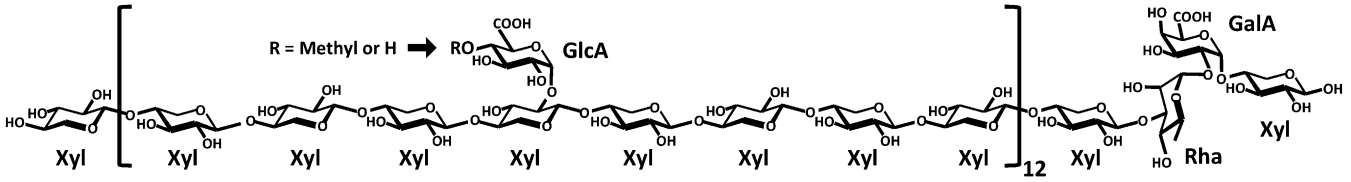


Fig. 1. Schematic structure of GX. *Arabidopsis* GX has a linear backbone of 1,4-linked β-D-Xyl residues. Approximately one in eight of these residues are substituted at *O*-2 with a single α-D-GlcA residue, which is usually modified by transfer of a methyl substituent to *O*-4 (arrow), forming a 4-*O*-methyl-α-D-GlcA (i.e., 4-*O*-MeGlcA) residue. The distinct reducing-end sequence shown is present in *Arabidopsis*, softwood and hardwood GXs (6).

molecular weight plant metabolites, which are involved in diverse biological processes that include signaling, defense, and lignin biosynthesis (21, 22). An early report also showed that the methyl group of SAM was also transferred to endogenous xylan in a cell-free system derived from corn cobs but the enzyme was not characterized (24).

Here, we provide genetic and biochemical evidence showing that an *Arabidopsis* gene (At1g33800) encodes a cation-dependent glucuronoxylan methyltransferase (GXMT) that specifically methylates *O*-4 of the GlcA substituents of GX. This OMT is a member of a family of proteins that contain a domain of unknown function 579 (DUF579). Functional characterization of AtGXMT1 as a polysaccharide specific OMT and the tools developed in this study provide new opportunities to understand the mechanisms of polysaccharide methylation, a largely unexplored aspect of polysaccharide biosynthesis.

Results and Discussion

Methyl-Etherification of GX Is Reduced in *GXMT1* Mutants. *Arabidopsis* proteins that contain a Pfam PF04669 domain (25), also known as DUF579, have been implicated in secondary cell wall development (15, 26–29). The DUF579 family includes four phylogenetic clades (Fig. S1*A*). Two genes (At1g33800 and At1g09610) encoding previously uncharacterized members of clade I (Fig. S2) are coexpressed with several other genes predicted to be involved in xylan synthesis, including *IRX7*, *IRX8*, *IRX9*, *IRX10*, *IRX15*, and *IRX15L* (15, 27, 28). To investigate the role of GXMT1 in GX biosynthesis we isolated and characterized two homozygous T-DNA insertional alleles (SALK_018081, *gxmt1-1*; SALK_087114, *gxmt1-2*) (Fig. S1*B*) in which At1g33800 is disrupted (Fig. S1*C*).

To identify and characterize changes in cell wall polysaccharide structure in *GXMT1* mutants, fractions enriched in pectic and hemicellulosic polysaccharides were isolated from mature inflorescence stems, which are rich in secondary cell walls. ^{1}H NMR spectroscopy (13) was used to compare the structures of the GX released by 1 N KOH-treatment of the alcohol insoluble residues (AIR) from inflorescence stems of wild-type, *gxmt1-1*, *gxmt1-2*, and *irregular xylem* 10 (*irx10*) plants. The *irx10* mutant has a well-established xylan chemotype (19) and served as a control. The ^{1}H-NMR spectra of the endo-xylanase–generated GX oligosaccharides (Fig. 2*A*) showed that the degree of GlcA *O*-methylation was 75% lower in both *gxmt1-1* and *gxmt1-2* plants than in wild-type plants and confirmed that GX produced by *irx10* has a reduced chain length and contains almost exclusively methylated GlcA (19). The amounts and distribution of branching and the degree of polymerization were indistinguishable for the GX from the *GXMT1* mutants and wild-type plants. Taken together,

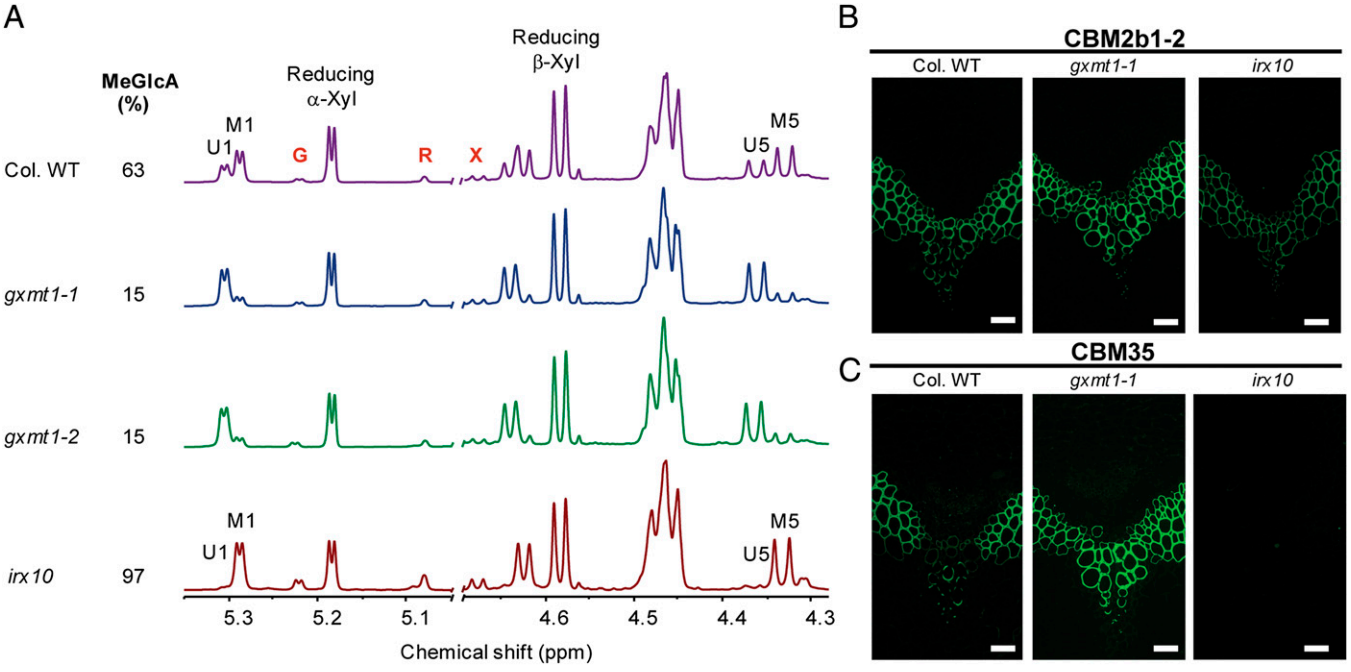


Fig. 2. *O*-methylation of GlcA is reduced in the GX produced by *GXMT1* mutants. (*A*) Partial 600-MHz ^{1}H NMR spectra of the oligosaccharides generated by endoxylanase treatment of the 1 N KOH-soluble GX from wild-type, *gxmt1-1*, *gxmt1-2*, and *irx10* stem cell walls. U1 is H1 of α-D-Glc*p*A, M1 is H1 of 4-*O*-methyl α-D-Glc*p*A, U5 is H5 of α-D-Glc*p*A, M5 is H5 of 4-*O*-methyl α-D-Glc*p*A, G is H1 of α-D-Gal*p*A, R is H1 of α-L-Rha*p*, and X is H1 of β-D-Xyl*p* linked to Rha. The extent of GlcA methylation was obtained by integration of U1 and M1. Indirect immunofluorescence microscopy of (*B*) CBM2b1-2 and (*C*) CBM35 binding to transverse sections of wild-type, *gxmt1-1*, and *irx10* stems. (Scale bars, 10 μm.)

Downloaded at ESKISEHIR OSMANGAZI UNIVERSITY on November 10, 2021

these data suggest that GXMT1 is involved in 4-*O*-methyl etherification of the GlcA residues of GX.

The pectic polysaccharide rhamnogalacturonan II contains 2-*O*-methyl-fucose and 2-*O*-methyl xylose (30). Comparable amounts of these methyl-etherified sugars were present in the pectic polysaccharides from *gxmt1-1* and wild-type plants (Fig. S3). Although 4-*O*-methyl-GlcA is known to be a component of arabinogalactan proteins in diverse plant species (31), we did not explore the effects of mutating *GXMT1* on the structures of these polymers. Of the polysaccharides we examined, GX is the only one whose O-methylation is affected in gxmt1-1 plants.

Although several *Arabidopsis* mutant lines, such as *irx10*, have altered xylan structure leading to collapsed xylem and interfascicular fibers with reduced wall thickness (13, 15, 18, 19), *gxmt1-1* stem sections are morphologically indistinguishable from wild-type stems (Fig. S4). Nevertheless, *gxmt1-1* stems contain GX that is distinct from wild-type GX, with reduced methylation as shown by cytochemical analysis using noncatalytic carbohydrate binding modules (CBM). One of these molecules, CBM2b1-2, which binds to the backbone of linear and substituted xylans (32), extensively labels the GX-rich secondary walls of interfascicular fibers and vascular bundles in both *gxmt1-1* and wild-type stems (Fig. 2*B*). As expected, less CBM2b1-2 labeling was observed in *irx10* stems (Fig. 2*B*), which display a collapsed xylem phenotype because of decreased amounts of GX (19). Conversely, CBM35 binds to GlcA but not to 4-*O*-methyl-GlcA substituents of GX (33). CBM35 and CBM2b1-2 displayed comparable labeling intensity in the walls of interfascicular fibers in the wild-type stems (Fig. 2 *B* and *C*). However, secondary walls of vascular xylem cells in these sections were weakly labeled with CBM35 (Fig. 2*C*), demonstrating that the GX in wild-type vascular xylem is highly methylated. Consistent with the almost complete methylation of GX in *irx10* walls (Fig. 2*A*), no binding of CBM35 was observed (Fig. 2*C*). Notably, all secondary walls of *gxmt1-1* stems were strongly labeled by CBM35. This binding was especially pronounced in xylem cells in vascular bundles (Fig. 2*C*), confirming that the GX in these tissues has a much lower degree of methylation relative to wild-type. These data are supported by analysis of transgenic *pGXMT1::GUS* lines (Fig. S5), which showed that the *GXMT1* promoter is active predominantly in vascular bundles of mature stems.

GXMT1 Is a GX-Specific Cation-Dependent 4-*O*-Methyltransferase. Our bioinformatic, spectroscopic, and histochemical analyses led us to hypothesize that GXMT1 is a GX methyltransferase. Thus, a recombinant tagged form of GXMT1 (amino acids 44–297) (Fig. S2) was expressed in *Escherichia coli*, purified and tested for its ability to transfer the methyl group from SAM to various acceptor substrates (Fig. S6*A*). Because it was not known if GlcA is methylated at the nucleotide sugar level or after its transfer to the xylan backbone, we evaluated a selection of potential GXMT1 acceptor substrates including GlcA, UDP-GlcA, and sparsely methylated GX isolated from the *gxmt1-1* mutant. After 48 h, the products formed were structurally characterized by 1D and 2D ^{1}H NMR spectroscopy to determine if *O*-methylation of the acceptor substrates had occurred. Our results establish that GXMT1 catalyzes the transfer of methyl groups exclusively to *O*-4 of GlcA in *gxmt1-1* GX and its fragment oligosaccharides (Fig. 3*A* and Fig. S7). No methyl groups were transferred to GlcA or UDP-GlcA (Fig. S7), indicating that methylation occurs after addition of GlcA to the xylan backbone. The rate of methyl transfer to polymeric *gxmt-1* xylan decreased after the first 3 h of the reaction (Fig. 3*A*) and after 48 h the degree of methylation had increased to 40%, which is somewhat less than the degree of methylation in wild-type GX. This result is likely due to inhibition by *S*-adenosyl-L-homocysteine (SAH), the end-product of the reaction and a strong competitive inhibitor of many SAM-dependent methyltransferases (34). Indeed, we found that in vitro GXMT1 activity is inhibited by adding SAH at the start of the reaction (Fig. S8). In vivo, plants use SAH hydrolase (EC 3.3.1.1) and adenosine kinase (EC 2.7.1.20) to metabolize SAH, thus circumventing its inhibitory effects and promoting SAM regeneration and methyltransferase activities (35).

To extend our knowledge regarding the biochemical properties of GXMT1, we adapted a liquid chromatography-electrospray ionization mass spectroscopy (LC-ESI-MS) method (36) to detect and quantify GX 4-*O*-methyltransferase activity. This technique, which quantifies a product of the OMT reaction (SAH) with a detection limit of 60.25 nM and a linear response up to 3 μM, was used to show that recombinant GXMT1 exhibits similar K_m and V_{max} values for GX and its oligosaccharide fragments (Fig. 3 *B* and *C*). The V_{max} and K_m can only be approximated, as the acceptor substrate is not soluble at concentrations above the estimated K_m.

Previous assays of xylan methyltransferase activity using crude microsomal membranes suggest that xylan methylation is enhanced by certain divalent cations and inhibited by EDTA (24, 37). We used the LC-ESI-MS–based assay to evaluate the 4-*O*-methyltransferase activity of metal-depleted GXMT1 in the presence of Co^{2+}, Sr^{2+}, Cu^{2+}, Mg^{2+}, Mn^{2+}, Ca^{2+} or EDTA. These analyses revealed that GXMT1-catalyzed transmethylation of GlcA substituents is a divalent metal-dependent process that is selectively potentiated by Co^{2+}, enhancing GXMT1 activity an average of 1,180%. Enzyme activity was completely inhibited by Cu^{2+} and EDTA (Fig. S6*B*). These data suggest that 4-*O*-methylation of GlcA proceeds via a catalytic mechanism characteristic of plant class I cation-dependent OMTs (23), consistent with an early report using a particulate enzyme from corn cobs (24). Plant cation-dependent OMTs typically require Mg^{2+}, Ca^{2+}, or Zn^{2+} for activity (38), although Co^{2+} can also enhance activity of selected OMTs (39). Although several cobalt-dependent mammalian DNA *N*-methyltransferases have been described (40), GXMT1 is the only Co^{2+}-dependent OMT described to date.

GXMT1 Is Localized in the Golgi Apparatus. GXs are believed to be synthesized in the Golgi apparatus, but it is not known if they are *O*-methylated in this organelle (8). Thus, we coexpressed GXMT1 fused to yellow fluorescent protein (GXMT1-YFP) with several well-characterized organelle markers in *Nicotiana benthamiana* and performed live-cell confocal analysis (41). GXMT1-YFP fluorescence, which was observed within small, highly mobile puncta characteristic of tobacco leaf Golgi (42), colocalized with the Golgi marker GmMan1-CFP (G-ck) (Fig. 3*D*), but not with the endoplasmic reticulum (ER) marker CFP-HDEL (ER-ck) or the plasma membrane (PM) marker AtPIP2A-CFP (pm-ck) (Fig. S9). The SVMtm transmembrane domain predictor (43) predicts that GXMT1 has a single transmembrane domain spanning amino acids 13–31. Taken together, these data suggest that xylan methylation occurs in the Golgi and is consistent with studies showing that other putative xylan biosynthetic enzymes are localized in this organelle (13, 19, 27, 28).

Potential Roles of Other DUF579 Proteins in Xylan Biosynthesis. IRX15 and IRX15L are two proteins in clade II of the DUF579 family (Fig. S1*A*) that have been proposed to be involved in GX biosynthesis, although their biochemical functions are not known (27, 28). IRX15 and IRX15L share low sequence similarity (30% identity) with GXMT1. Nevertheless, several of the amino acid sequences predicted to function in divalent metal coordination and SAM/SAH binding are conserved in IRX15 and IRX15L, indicating that these proteins may function as OMTs (Fig. S2). However, a direct role for IRX15 and IRX15L in *O*-methylation of GX is difficult to reconcile with the observation that the degree of GlcA *O*-methylation is increased in *irx15* and *irx15l* single mutants, and that the *irx15 irx15l* double mutant (27) produces a homodisperse, highly methylated GX with a reduced degree of polymerization (27, 28), similar to that found in *irx9* and *irx10* mutants. IRX9 and IRX10 are members of GT families GT43 and GT47, respectively, and have been implicated in xylan backbone elongation (13, 19). Thus, the possibility cannot be discounted that IRX15 and IRX15L are structural rather than catalytic components of a putative xylan synthase complex. Noncatalytic GT homologs have been proposed to participate in the assembly of GT complexes involved in pectin synthesis (44). IRX15 and IRX15L may serve a similar role in xylan biosynthesis.

Downloaded at ESKISEHIR OSMANGAZI UNIVERSITY on November 10, 2021

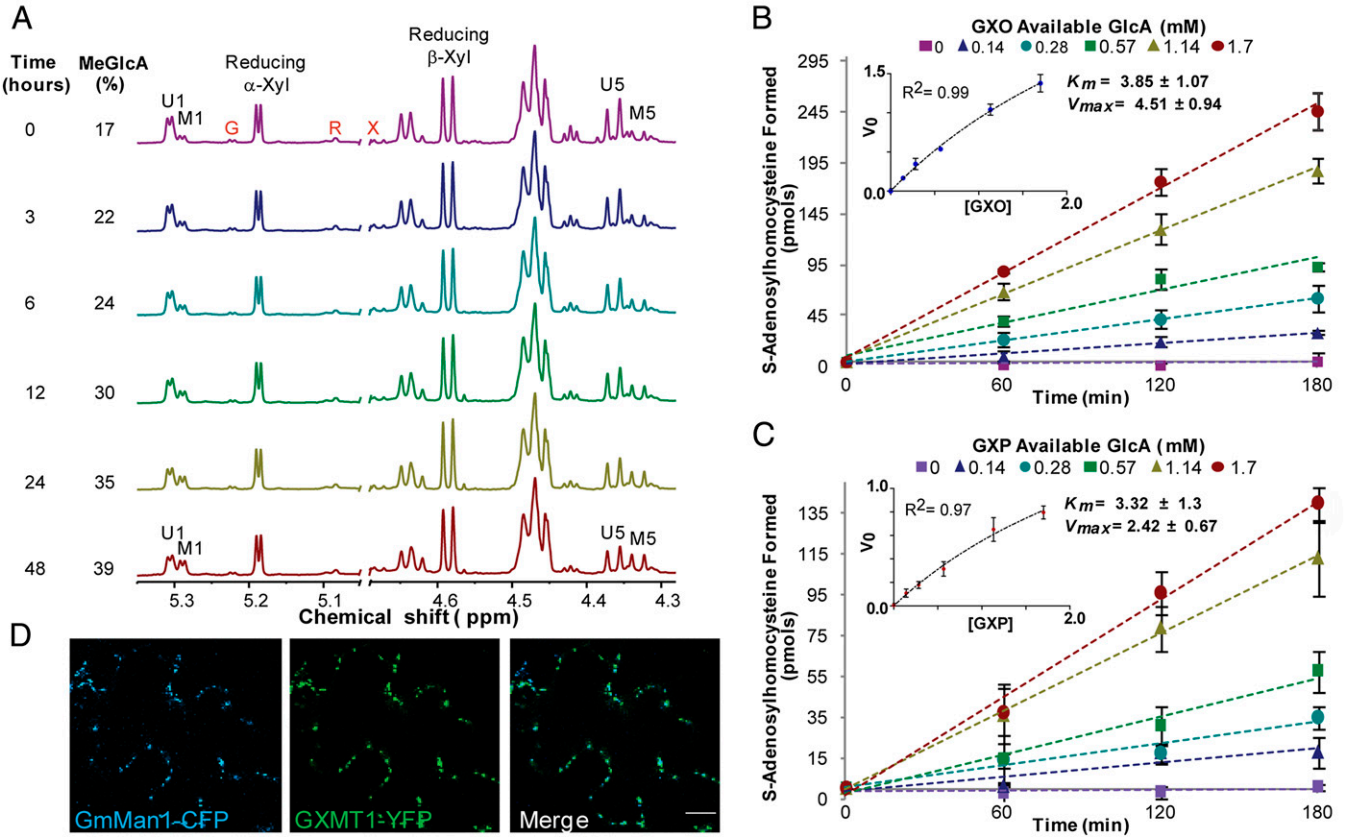


Fig. 3. Heterologously expressed GXMT1 catalyzes 4-*O*-methylation of GX in vitro and is located in the Golgi. (*A*) ^{1}H NMR spectra of the oligosaccharides generated by endoxylanase treatment of the products formed when *gxmt1-1* GX was incubated with GXMT1 and SAM. GlcA *O*-methylation was quantified by integration of signals labeled U1 and M1 (see Fig. 2). Kinetics of methyl transfer to (*B*) oligomeric (GXO) or (*C*) polymeric (GXP) *gxmt1-1* GX as determined by measuring the amounts of SAH formed upon transfer of the methyl group from SAM in the presence of GXMT1 (340 pmol). Error bars are ± SD, $n = 3$. Kinetic constants K_m (mM) and V_{max} (pmol SAH min^{-1}) were calculated by fitting the initial velocities (V_0, pmol SAH min^{-1}) as a function of the acceptor substrate concentration (GXO) or (GXP) (millimolar) to the Michaelis-Menten equation using nonlinear curve fitting (*Inset*). (*D*) Subcellular localization of transiently expressed GXMT1-YFP in *N. benthamiana* epidermal cells observed by confocal laser-scanning microscopy. Coexpression of CFP-tagged Golgi apparatus marker (GmMan1-CFP, G-ck; *Left*) and GXMT1-YFP (*Center*) shows GXMT1-YFP is colocalized with the Golgi marker in the merged image (*Right*). (Scale Bar, 20 μm.)

Mutating *GXMT1* Enhances Xylan Release During Mild Hydrothermal Pretreatment. Engineering plant biomass to increase the accessibility of secondary cell wall components to enzyme-catalyzed hydrolysis may facilitate the conversion of biomass into fermentable sugars (4, 5). One promising approach is to alter the expression of genes that affect the molecular interactions of polymers responsible for the wall's structural integrity. For example, modulating the expression of OMTs involved in lignin biosynthesis has had success in decreasing the recalcitrance of plant biomass to enzyme-catalyzed saccharification (45, 46). In contrast, the effects of manipulating *O*-methylation of GX are unknown. We therefore examined the effects of reduced *O*-methylation of GX on the release of xylose during hydrothermal pretreatment at several severities (47). Wild-type and *gxmt1-1* plants contain comparable amounts of total glucan and xylan (Fig. 4*A*). However, hydrothermal pretreatment solubilized more xylan from *gxmt1-1* AIR than from wild-type AIR (Fig. 4*B*). This difference was greatest when the least-severe condition (11.1 min) was used. When this pretreatment was followed by cellulase and xylanase treatments, a greater proportion of the xylose and more total sugar were released from the *gxmt1-1* AIR than from wild-type AIR (Fig. 4*C*). These data suggest that the molecular interactions holding GX in secondary walls are altered in *gxmt1-1* plants and that mild hydrothermal pretreatment protocols that efficiently remove GX from such plants are feasible. Harsh pretreatments using mineral acids or high temperatures for extended times typically convert some of the GX to by-products that inhibit downstream processing by enzymes or microorganisms (48). Thus, biomass engineered to facilitate GX solubilization using mild hydrothermal conditions has potential as a feedstock that can be efficiently converted to fermentable sugars.

The selective removal of GX from biomass can be enhanced by using glycanases engineered to contain CBMs that target this polysaccharide (49). In this context, we demonstrated that a bacterial xylanase (Xyl10B) linked to CBM35 is more effective than the xylanase alone in fragmenting GX in the secondary cell walls of *gxmt1-1* plants (Fig. S10). These results establish proof-of-principle for approaches that combine engineered secondary cell walls with designer endoglycanases to increase the efficiency of bioconversion technologies for lignocellulosic feedstocks.

Mutation of *GXMT1* Results in Altered Lignin Structure. Patten et al. (50) observed that the S-lignin is less abundant in *Arabidopsis* stem vascular bundles than in interfascicular fibers. Our data (Fig. 2 *B* and *C*) indicate that the degree of *O*-methylation of GX is higher in vascular bundles than in interfascicular fibers. This finding suggests that the degree of GX methylation is negatively correlated to the degree of lignin methylation. Indeed, HSQC NMR spectroscopy (51) showed that the decrease in *O*-methylation of GX in *gxmt1-1* plants is correlated to a ~20% increase in the overall extent of lignin methylation, manifested as an increase in S lignin and a decrease in H lignin (Fig. 4 *D* and *E*). GX

Downloaded at ESKISEHIR OSMANGAZI UNIVERSITY on November 10, 2021

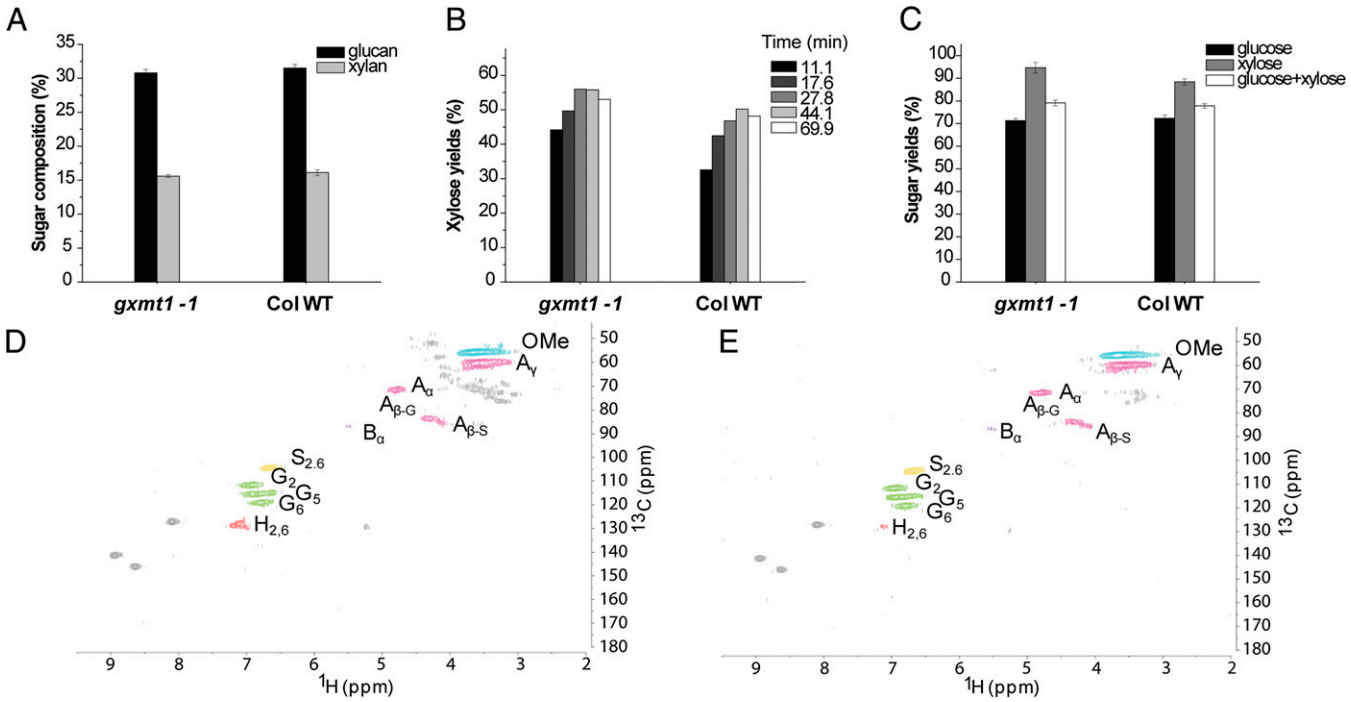


Fig. 4. Hydrothermal pretreatment releases more xylose from *gxmt1-1* biomass than from wild-type biomass. (*A*) Glucan and xylan contents of *Arabidopsis* wild-type and *gxmt1-1* stem biomass. (*B*) Total xylose (monomer plus oligomers) released during hydrothermal pretreatment at 180 °C for the specified times (min). (*C*) Glucose, xylose and total glucose plus xylose released by cellulase and xylanase (150 mg protein/g structural sugars in biomass) after hydrothermal pretreatment (180 °C for 11.1 min). Error bars are SD $n = 3$. HSQC spectra of the lignin-enriched material from wild-type (*D*) and *gxmt1-1* (*E*) stems reveal subtle structural differences. HSQC cross-peak assignments are annotated using the nomenclature of Kim and Ralph (51). Resonance assignments: A, various monolignols connected by β-O4 linkages; B, monolignols connected by phenylcoumaran linkages; G, guaiacyl residues; S, syringyl residues; H, hydroxyphenyl residues; OMe, phenolic methoxyl groups. Specific atom assignments are indicated by subscript numbers or Greek letters.

and lignin biosynthesis compete for a limited pool of SAM that is available during secondary cell wall synthesis. Therefore, the increase in lignin methylation observed in *gxmt1-1* plants may reflect changes in metabolic flux associated with the decrease in GX methylation. Alternatively, *O*-methylation of GX may influence its association with the amphiphilic surface of lignin or the monolignols from which lignin is polymerized, thereby exerting a direct effect on lignin assembly in the cell wall.

Conclusions

We have shown that *Arabidopsis GXMT1* encodes a GX-specific 4-*O*-methyltransferase responsible for methylating 75% of the GlcA residues in GX isolated from mature *Arabidopsis* inflorescence stems. Reduced methylation of GX in *gxmt1-1* plants is correlated with altered lignin composition and increased release of GX by mild hydrothermal pretreatment. In addition to providing fundamental insights into cell wall synthesis, our discovery and characterization of AtGXMT1 extends the portfolio of structural targets that can be modified either alone or in combination to increase the economic value of lignocellulosic biomass. The ability to selectively manipulate polysaccharide *O*-methylation may provide new opportunities to modulate biopolymer interactions in the plant cell wall. The implications of our discovery are not limited to xylan biosynthesis, as other members of the DUF579 family may well catalyze the methyletherification of other plant polysaccharides.

Materials and Methods

Plant Materials and Mutant Identification. All *A. thaliana* plants were in the Columbia (Col-0) background. Seeds of T-DNA insertion lines (SALK_018081, *gxmt1-1*; SALK_087114, *gxmt1-2*) were obtained from the *Arabidopsis* Biological Resource Center (www.arabidopsis.org). Plants were grown for 8 wk under short-day conditions (12-h photoperiod) at 22 °C, 50% relative humidity, and a light intensity of ~180 μmol photons $m^{-2}{\cdot}s^{-1}$. (For details, see *SI Materials and Methods*).

Preparation and Analysis of Cell Wall Polysaccharides. Details of cell wall preparation and analyses are described in *SI Materials and Methods*.

Generation of GST-GXMT1 Fusion Protein. The GXMT1 protein was expressed in *E. coli* BL21-CodonPlus (DE3)-RIPL cells with an N-terminal GST tag (GST-GXMT1). Details of generation, expression and purification of the GST-GXMT1 fusion protein are described in *SI Materials and Methods*.

Determination of Methyltransferase Activity Using ^{1}H-NMR Spectroscopy and LC-ESI-MS. The temperature optimum for GXMT1 activity was between 19–25 °C (Fig. S6*C*). The transfer of methyl groups to *O*-4 of GlcA was established by ^{1}H NMR spectroscopy. Assays were performed at 23 °C in 50 mM potassium bicarbonate, pH 7.5, (250 μL) containing acceptor substrate equivalent to 2.27 mM available GlcA residues, recombinant GXMT1 (10 μM), $CoCl_2$ (2 mM), and 1.5 mM S-adenosyl-L-methionine sulfate *p*-toluenesulfonate (SAMe-PTS), unless otherwise indicated. The formation of SAH from SAM was determined using LC-ESI-MS (36). Assays were performed in 50 mM Hepes, pH 7.5 (100 μL) with recombinant GXMT1 (3.4 μM), *gxmt1-1* xylan polymer (220 μg), $CoCl_2$ (1 mM), and various amounts of SAMe-PTS. Details of both assays are in *SI Materials and Methods*.

Subcellular Localization of GXMT1. Vector construction for the N-terminal fusion of GXMT1 to YFP, transient expression in *N. benthamiana*, and confocal microscopy are described in *SI Materials and Methods*. Marker proteins for ER (ER-ck), Golgi apparatus (G-ck), and PM (pm-ck) fused to CFP have been described previously (41).

Glucose and Xylose Release from *Arabidopsis* AIR by Hydrothermal Pretreatment and Enzymatic Hydrolysis. The amounts of glucan and xylan in *Arabidopsis* stem AIR were determined as previously described (52). Hydrothermal pretreat-

Downloaded at ESKISEHIR OSMANGAZI UNIVERSITY on November 10, 2021

ment and enzymatic hydrolysis of *Arabidopsis* stem AIR were performed as described in *SI Materials and Methods*.

Determination of the Lignin Monomer Composition of *Arabidopsis* AIR by HSQC NMR Spectroscopy. AIR from ball-milled *Arabidopsis* stems was used for the preparation of the lignin enriched material for NMR analyses. See *SI Materials and Methods* for details.

Indirect Immunofluorescence Microscopy of *Arabidopsis* Stems Using Xylan Binding Modules as Molecular Probes. Previously published protocols were used to construct, express, and purify CBM35 (53) and CBM2b-1–2 (54). Tissue preparation, CBM labeling, and microscopy of 6-wk-old *Arabidopsis* stem sections were as previously described (55). Details are in *SI Materials and Methods*.

ACKNOWLEDGMENTS. We thank Ron Clay for assistance with β-glucuronidase staining. This work was supported in part by US Department of Energy Grants DE–FG02–93ER20097 (to A.G.D.) for the Department of Energy-funded Center for Plant and Microbial Complex Carbohydrates, and DE-FG02-09ER16076 (to H.J.G.) for studies of plant carbohydrate binding modules; and by National Institutes of Health Grant 1R01GM086524-01 (to H.F.S.) for confocal microscopy. The BioEnergy Science Center is a US Department of Energy Bioenergy Research Center supported by the Office of Biological and Environmental Research in the Department of Energy Office of Science.

1. Niklas KJ (1997) *The Evolutionary Biology of Plants* (Univ of Chicago Press, Chicago).
2. Petersen RC (1984) The chemical composition of wood. *The Chemistry of Solid Wood*, ed Rowell RM (American Chemical Society, Washington, DC), pp 57–126.
3. Jung HG, Allen MS (1995) Characteristics of plant cell walls affecting intake and digestibility of forages by ruminants. *J Anim Sci* 73:2774–2790.
4. Carroll A, Somerville C (2009) Cellulosic biofuels. *Annu Rev Plant Biol* 60:165–182.
5. Himmel ME, et al. (2007) Biomass recalcitrance: Engineering plants and enzymes for biofuels production. *Science* 315:804–807.
6. York WS, O'Neill MA (2008) Biochemical control of xylan biosynthesis—Which end is up? *Curr Opin Plant Biol* 11:258–265.
7. Sandhu APS, Randhawa GS, Dhugga KS (2009) Plant cell wall matrix polysaccharide biosynthesis. *Mol Plant* 2:840–850.
8. Scheller HV, Ulvskov P (2010) Hemicelluloses. *Annu Rev Plant Biol* 61:263–289.
9. Somerville C (2006) Cellulose synthesis in higher plants. *Annu Rev Cell Dev Biol* 22: 53–78.
10. Vanholme R, Demedts B, Morreel K, Ralph J, Boerjan W (2010) Lignin biosynthesis and structure. *Plant Physiol* 153:895–905.
11. Wang HZ, Dixon RA (2012) On-off switches for secondary cell wall biosynthesis. *Mol Plant* 5:297–303.
12. Ebringerova A, Hromadkova Z, Heinze T (2005) Hemicellulose. *Adv Polym Sci* 186: 1–67.
13. Peña MJ, et al. (2007) Arabidopsis *irregular xylem8* and *irregular xylem9*: Implications for the complexity of glucuronoxylan biosynthesis. *Plant Cell* 19:549–563.
14. Kulkarni AR, et al. (2012) The ability of land plants to synthesize glucuronoxylans predates the evolution of tracheophytes. *Glycobiology* 22:439–451.
15. Brown DM, Zeef LA, Ellis J, Goodacre R, Turner SR (2005) Identification of novel genes in *Arabidopsis* involved in secondary cell wall formation using expression profiling and reverse genetics. *Plant Cell* 17:2281–2295.
16. Zhong R, et al. (2005) *Arabidopsis fragile fiber8*, which encodes a putative glucuronyltransferase, is essential for normal secondary wall synthesis. *Plant Cell* 17: 3390–3408.
17. Rennie E, et al. (2012) Three members of the *Arabidopsis* glycosyltransferase family 8 are xylan glucuronosyltransferases. *Plant Physiol*, 10.1104/pp.112.200964.
18. Brown DM, et al. (2007) Comparison of five xylan synthesis mutants reveals new insight into the mechanisms of xylan synthesis. *Plant J* 52:1154–1168.
19. Wu AM, et al. (2009) The *Arabidopsis* IRX10 and IRX10-LIKE glycosyltransferases are critical for glucuronoxylan biosynthesis during secondary cell wall formation. *Plant J* 57:718–731.
20. Mortimer JC, et al. (2010) Absence of branches from xylan in *Arabidopsis gux* mutants reveals potential for simplification of lignocellulosic biomass. *Proc Natl Acad Sci USA* 107:17409–17414.
21. Ibrahim RK, Bruneau A, Bantignies B (1998) Plant *O*-methyltransferases: molecular analysis, common signature and classification. *Plant Mol Biol* 36:1–10.
22. Lam KC, Ibrahim RK, Behdad B, Dayanandan S (2007) Structure, function, and evolution of plant *O*-methyltransferases. *Genome* 50:1001–1013.
23. Kopycki JG, et al. (2008) Biochemical and structural analysis of substrate promiscuity in plant Mg^{2+}-dependent *O*-methyltransferases. *J Mol Biol* 378:154–164.
24. Kauss H, Hassid WZ (1967) Biosynthesis of the 4-*O*-methyl-D-glucuronic acid unit of hemicellulose B by transmethylation from S-adenosyl-L-methionine. *J Biol Chem* 242: 1680–1684.
25. Finn RD, et al. (2010) The Pfam protein families database. *Nucleic Acids Res* 38(Database issue):D211–D222.
26. Oikawa A, et al. (2010) An integrative approach to the identification of *Arabidopsis* and rice genes involved in xylan and secondary wall development. *PLoS ONE* 5: e15481.
27. Brown D, et al. (2011) *Arabidopsis* genes *IRREGULAR XYLEM (IRX15)* and *IRX15L* encode DUF579-containing proteins that are essential for normal xylan deposition in the secondary cell wall. *Plant J* 66:401–413.
28. Jensen JK, et al. (2011) The DUF579 domain containing proteins IRX15 and IRX15-L affect xylan synthesis in *Arabidopsis*. *Plant J* 66:387–400.
29. Ruprecht C, et al. (2011) Large-scale co-expression approach to dissect secondary cell wall formation across plant species. *Front Plant Sci* 2:23.
30. O'Neill MA, Ishii T, Albersheim P, Darvill AG (2004) Rhamnogalacturonan II: Structure and function of a borate cross-linked cell wall pectic polysaccharide. *Annu Rev Plant Biol* 55:109–139.
31. Gaspar Y, Johnson KL, McKenna JA, Bacic A, Schultz CJ (2001) The complex structures of arabinogalactan-proteins and the journey towards understanding function. *Plant Mol Biol* 47:161–176.
32. McCartney L, et al. (2006) Differential recognition of plant cell walls by microbial xylan-specific carbohydrate-binding modules. *Proc Natl Acad Sci USA* 103:4765–4770.
33. Montanier C, et al. (2009) Evidence that family 35 carbohydrate binding modules display conserved specificity but divergent function. *Proc Natl Acad Sci USA* 106: 3065–3070.
34. Moffatt BA, Weretilnyk EA (2001) Sustaining S-adenosyl-L-methionine-dependent methyltransferase activity in plant cells. *Physiol Plant* 113:435–442.
35. Pereira LA, et al. (2007) Methyl recycling activities are co-ordinately regulated during plant development. *J Exp Bot* 58:1083–1098.
36. Salyan MEK, et al. (2006) A general liquid chromatography/mass spectroscopy-based assay for detection and quantitation of methyltransferase activity. *Anal Biochem* 349: 112–117.
37. Baydoun EA, Waldron KW, Brett CT (1989) The interaction of xylosyltransferase and glucuronyltransferase involved in glucuronoxylan synthesis in pea (*Pisum sativum*) epicotyls. *Biochem J* 257:853–858.
38. Ferrer JL, Zubieta C, Dixon RA, Noel JP (2005) Crystal structures of alfalfa caffeoyl coenzyme A 3-*O*-methyltransferase. *Plant Physiol* 137:1009–1017.
39. Lukačin R, Matern U, Specker S, Vogt T (2004) Cations modulate the substrate specificity of bifunctional class I *O*-methyltransferase from *Ammi majus*. *FEBS Lett* 577: 367–370.
40. Pfohl-Leszkowicz A, Baldacini O, Keith G, Dirheimer G (1987) Stimulation of rat kidney, spleen and brain DNA-(cytosine-5-)-methyltransferases by divalent cobalt ions. *Biochimie* 69:1235–1242.
41. Nelson BK, Cai X, Nebenführ A (2007) A multicolored set of in vivo organelle markers for co-localization studies in *Arabidopsis* and other plants. *Plant J* 51:1126–1136.
42. Brandizzi F, Snapp EL, Roberts AG, Lippincott-Schwartz J, Hawes C (2002) Membrane protein transport between the endoplasmic reticulum and the Golgi in tobacco leaves is energy dependent but cytoskeleton independent: Evidence from selective photobleaching. *Plant Cell* 14:1293–1309.
43. Yuan Z, Mattick JS, Teasdale RD (2004) SVMtm: support vector machines to predict transmembrane segments. *J Comput Chem* 25:632–636.
44. Atmodjo MA, et al. (2011) Galacturonosyltransferase (GAUT)1 and GAUT7 are the core of a plant cell wall pectin biosynthetic homogalacturonan:galacturonosyltransferase complex. *Proc Natl Acad Sci USA* 108:20225–20230.
45. Chen F, Dixon RA (2007) Lignin modification improves fermentable sugar yields for biofuel production. *Nat Biotechnol* 25:759–761.
46. Fu C, et al. (2011) Genetic manipulation of lignin reduces recalcitrance and improves ethanol production from switchgrass. *Proc Natl Acad Sci USA* 108:3803–3808.
47. Studer MH, DeMartini JD, Brethauer S, McKenzie HL, Wyman CE (2010) Engineering of a high-throughput screening system to identify cellulosic biomass, pretreatments, and enzyme formulations that enhance sugar release. *Biotechnol Bioeng* 105: 231–238.
48. Mosier N, et al. (2005) Features of promising technologies for pretreatment of lignocellulosic biomass. *Bioresour Technol* 96:673–686.
49. Hervé C, et al. (2010) Carbohydrate-binding modules promote the enzymatic deconstruction of intact plant cell walls by targeting and proximity effects. *Proc Natl Acad Sci USA* 107:15293–15298.
50. Patten AM, et al. (2010) Probing native lignin macromolecular configuration in *Arabidopsis thaliana* in specific cell wall types: Further insights into limited substrate degeneracy and assembly of the lignins of *ref8, fah 1-2* and *C4H:F5H* lines. *Mol Biosyst* 6:499–515.
51. Kim H, Ralph J (2010) Solution-state 2D NMR of ball-milled plant cell wall gels in DMSO-d(6)/pyridine-d(5). *Org Biomol Chem* 8:576–591.
52. DeMartini JD, Studer MH, Wyman CE (2011) Small-scale and automatable high-throughput compositional analysis of biomass. *Biotechnol Bioeng* 108:306–312.
53. Bolam DN, et al. (2004) X4 modules represent a new family of carbohydrate-binding modules that display novel properties. *J Biol Chem* 279:22953–22963.
54. Bolam DN, et al. (2001) Evidence for synergy between family 2b carbohydrate binding modules in *Cellulomonas fimi* xylanase 11A. *Biochemistry* 40:2468–2477.
55. Pattathil S, et al. (2010) A comprehensive toolkit of plant cell wall glycan-directed monoclonal antibodies. *Plant Physiol* 153:514–525.

Downloaded at ESKISEHIR OSMANGAZI UNIVERSITY on November 10, 2021